PERGAMON

Vision Research 38 (1998) 3117–3128

Vision Research

Spectral bandwidths for the detection of color

Michael D'Zmura *, Kenneth Knoblauch

Institut d'Ingéniérie de la Vision, Université Jean Monnet de Saint-Etienne, France

Received 14 July 1997; received in revised form 15 September 1997

Abstract

The spectral properties of human color detection mechanisms were measured using a noise masking technique that minimizes the possibility of off-axis looking and artifactually narrow estimates of bandwidth. Observers were induced to use a single detection mechanism throughout a spectral bandwidth measurement by using sectored noise to mask a time-varying signal of fixed chromatic properties. Sectored noise draws samples from sectors of variable width in the color plane, centered on the signal axis. Contrast thresholds for equiluminant signals that appeared yellow, orange, red and violet were found to depend on the power of the noise, projected along the chromatic axis of the signal, but not on the sector width of the noise. These results are consistent with the activity of spectrally broadband, linear detection mechanisms that are tuned to the signal color directions tested.

Keywords: Color; Noise; Detection; Sensitivity; Masking

1. Introduction

Recent studies of the spectral sensitivities of color detection mechanisms have focused on two questions. The first is whether there are detection mechanisms with spectral sensitivities that lie between those of the three standard mechanisms—the black–white, the red–green and the yellow–blue [1]. Results of psychophysical work with habituation [2], visual search [3,4] and noise masking [5] suggest strongly that such mechanisms exist and operate in everyday visual detection tasks. For example, the findings show that observers can deploy an orange-sensitive mechanism when looking for an orange signal rather than looking for simultaneous red and yellow events.

These psychophysical studies are supported by the results of electro-physiological experiments on neurons in the visual pathways of macaque monkeys. While the spectral sensitivities of neurons in LGN tend to cluster about two axes in the color plane [6,7], neurons in cortical areas V1 [8,9], V2 [10] and V3 [11] have spectral sensitivities which are scattered more uniformly within the color plane. Many color-sensitive neurons are found in visual cortex which are most sensitive to hues that lie between the axes that characterize retinogeniculate processing.

A second issue is whether color detection mechanisms have broad or narrow spectral sensitivities. Broad sensitivities are consistent with the combination of cone photoreceptoral inputs in a spectrally linear fashion, while narrow sensitivities can only be created through non-linear combination. The electro-physiological studies report that the majority of color-sensitive neurons combine cone signals linearly, with the possible exception of some form of rectification linked to low levels of maintained discharge [7,8]. However, cortical neurons with narrowband spectral tuning have been found [8,10].

In this paper we report the results of psychophysical experiments in which a sectored noise masking technique is used to measure the spectral bandwidths of color detection mechanisms. With this method, noise chromaticities are chosen to fill a sector within color space that is centered along the chromatic axis of the signal. The sector has an amplitude and a width that are under experimental control. By measuring the potency of noise masking as a function of sector width, one can distinguish directly between the broad sensitiv-

* Corresponding author. Present address: Department of Cognitive Sciences, University of California, Irvine, Irvine, CA 92697, USA. Tel.: +1 949 8244055; fax: +1 949 8242663; e-mail: mdzmura@uci.edu.

0042-6989/98/$19.00
PII: S0042-6989(97)00381-7

ities of linear mechanisms and narrowband sensitivities. The sensitivity of a linear mechanism to sectored noise that is centered on the peak axis of the mechanism is independent of sector width. Noise masking potency will decline with increasing sector width if the detection mechanism has a narrowband sensitivity.

This work with sectored noise applies techniques that were developed earlier in studies of 'critical bands' in audition [12] and in spatial vision [13]. The present results for color vision show that noise masking is independent of sector width, for signals that appear yellow, orange, red and violet. One infers that color detection is served by mechanisms tuned to a variety of directions in color space, and that these mechanisms have broad, linear spectral sensitivities [14]. Preliminary reports of this work were made by D'Zmura and Knoblauch [15,16].

2. Methods

The task of observers was to detect an equiluminant chromatic pulse with a Gaussian time-course, presented within time-varying noise. The signal pulse and the noise were used to modulate the appearance of a spatially Gaussian blob, displayed in the center of a color monitor set to a neutral gray. Noise properties were varied systematically to measure the spectral sensitivity of the signal detection mechanism.

2.1. Equipment

Stimuli were presented on an Eizo FlexScan T562-T color monitor that observers viewed binocularly at a distance of 0.56 m in a dark room. Software on a Compaq Prolinea 486 controlled a Cambridge Research Systems VSG/2 color graphics board that provided 12 bits of chromatic information for each of the 800 wide $\times$ 600 high pixels presented on the monitor. The non-linear relationship between applied voltage and phosphor intensity was corrected, for each gun, using color look-up tables. The chromaticities and luminances of the three phosphors of the monitor were measured using a Minolta CS-100 chromameter. The screen was set to display a steady, neutral gray background with luminance 65 cd/m^2 and a chromaticity (0.294, 0.303) for the CIE 1931 standard observer.

2.2. Observers

The measurements reported here were made by three color-normal observers. One of these was an author (MD); the other two observers (FM and RY) were naïve as to the purpose of the experiments.

2.3. Color space

The color properties of stimuli are described in the DKL color space [7], which is based on the MacLeod and Boynton [17] color diagram. This color space, shown in Fig. 1, is related to the LMS cone contrast space by a linear transformation [18]. Features in this space are defined relative to the gray point **G**, which serves in these experiments as the neutral light to which the visual system remains adapted.

The color space has three cardinal axes [19] that intersect at the gray point (see Fig. 1). The first is the achromatic or black–white axis; lights along this axis are created by generating equal modulations of the three phosphors about the gray point and differ in brightness. The other two cardinal axes lie in the equiluminant plane through the gray point **G**; all lights in this plane are of equal luminance as defined by the V_λ photopic luminosity function [20]. Modulation along the L and M cone axis (red/blue–green) changes the excitations of L and M cones and is invisible to S cones. Modulation along the S cone axis (yellow–green/purple) changes the excitation of S cones and is invisible to both L and M cones. Assuming that S cones make no contribution to luminosity [21], then the S cone axis is the tritanopic confusion line through the gray point. The L and M cone and S cone axes are perpendicular in this color space and in the LMS color space of contrasts to individual cone mechanisms.

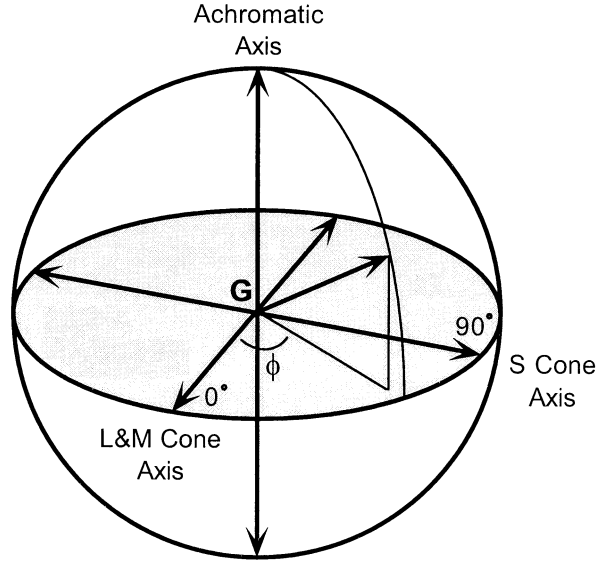

Fig. 1. Color space of Derrington et al. [7]. The L and M cone axis and the S cone axis define an equiluminant plane that is centered on the neutral gray point **G**. The direction of a vector in the equiluminant plane may be specified by its azimuth ϕ. The 'red' half of the L and M cone axis is assigned arbitrarily an azimuth of 0° and the 'yellow–green' half of the S cone axis an azimuth of 90°. The achromatic axis passes through the equiluminant plane at **G**.

A light may be represented in the DKL color space as a vector based at the gray point **G**. The vector can be described in several ways. One may use Cartesian co-ordinates, where the vector components are the projections of the vector onto the L and M cone, S cone and achromatic axes. We arbitrarily define the unit vectors along the L and M cone axis and the S cone axis to present contrasts of 0.021 and 0.89 to L cones and S cones, respectively. An alternative is to use a spherical co-ordinate system that is centered on the gray point. The co-ordinates of a vector are then (1) its azimuth, which is found by projecting the vector onto the equiluminant plane and then measuring the angle between the projection and the 'red' half of the L and M cone axis (which has an arbitrarily-set azimuth of 0°); (2) its elevation, which is the angle between the original vector and the 'white' end of the achromatic axis, which describes the achromatic contrast of the light, and (3) its length, which describes the amount of contrast presented by the light to a mechanism that lies along the vector's axis. For lights that lie in the equiluminant plane, azimuth is an index of hue and length is related to chromatic contrast or saturation.

3. Description of linear mechanisms

The relative spectral sensitivity of a mechanism that combines linearly signals from cones may be displayed in the color space in several ways. A linear mechanism can be characterized by its null plane [7], which is the set of lights, including the gray point **G**, that stimulates the mechanism to the same extent that the gray point does. Modulation among any lights that lie within the null plane is invisible to the mechanism. Parallel to a null plane lie what may be called response level sets. All lights that lie in a single such set give rise to responses of identical strength. The null plane is a level set of response zero. The null plane and non-zero response level sets of a linear color-opponent mechanism are lines when plotted in the equiluminant plane of Fig. 1. Fig. 2 shows the null axis and several response level sets for a hypothetical red–green mechanism that opposes inputs from L and M cones and receives input from S cones of the same sign as that from L cones [22–24].

The response level set characterization is equivalent to a gradient or 'best axis' characterization [8]. The most effective lights to use in stimulating a linear mechanism lie along an axis that is perpendicular to the response level sets of the mechanism (Fig. 2). If the mechanism is completely linear, then it can be specified by just three numbers, namely the co-ordinates of the gradient vector. The response r of a linear mechanism with gradient vector $\boldsymbol{m}$ to a stimulus represented by vector $\boldsymbol{w}$ is the dot product of the two vectors:

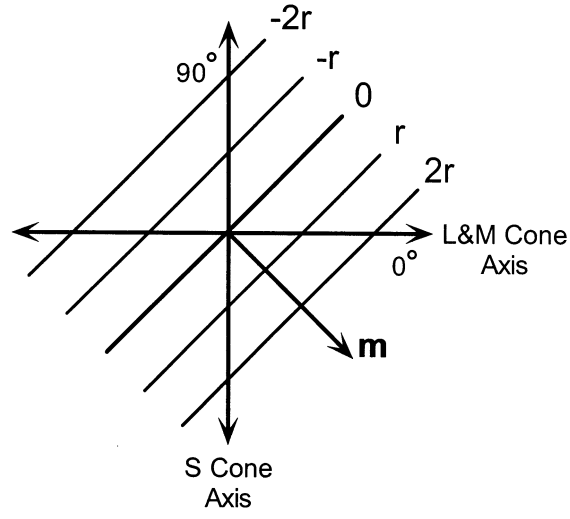

Fig. 2. Response level sets for a mechanism that opposes L and M cones and receives input from S cones of the same sign as that from L cones. This linear mechanism is represented, in the equiluminant plane, by a stack of lines parallel to the null axis (response 0) that describe the contrast vectors that lead to identical responses r, $2r$, etc. An opponent mechanism also has negative response level sets. The gradient $\boldsymbol{m}$ that runs perpendicularly through this stack represents the peak spectral sensitivity of the mechanism.

$$r = \boldsymbol{m}^{\mathrm{T}} \cdot \boldsymbol{w}. \tag{1}$$

Response level sets are determined by finding the set $\mathscr{W}_c$ of stimuli that produce some constant level of response c:

$$c = \boldsymbol{m}^{\mathrm{T}} \cdot \boldsymbol{w}, \quad \boldsymbol{w} \in \mathscr{W}_c. \tag{2}$$

Setting c to zero produces the null plane. The azimuth and elevation of the gradient vector specify the relative spectral sensitivity of the mechanism, while the length of the gradient vector specifies its absolute sensitivity to modulations about the gray point [25].

3.1. Stimuli

Observers viewed a gray uniform field that was displayed on the color monitor. A colored patch in the form of a spatially isotropic Gaussian function with space constant 2.4° of visual angle was presented in the center of the field. Signal and noise, with chromatic properties that could be chosen independently of one another, were used together to modulate in time the chromaticity of the central patch. The temporal and chromatic properties of the stimuli are shown in Fig. 3.

3.1.1. Signal

Signals had a Gaussian time-course with a time constant of 160 ms and a duration of 640 ms; the signals were truncated at ± 2 S.D. Such signals are mono-polar modulations of chromaticity from the gray point. The contrast of the signal at its peak is used as a

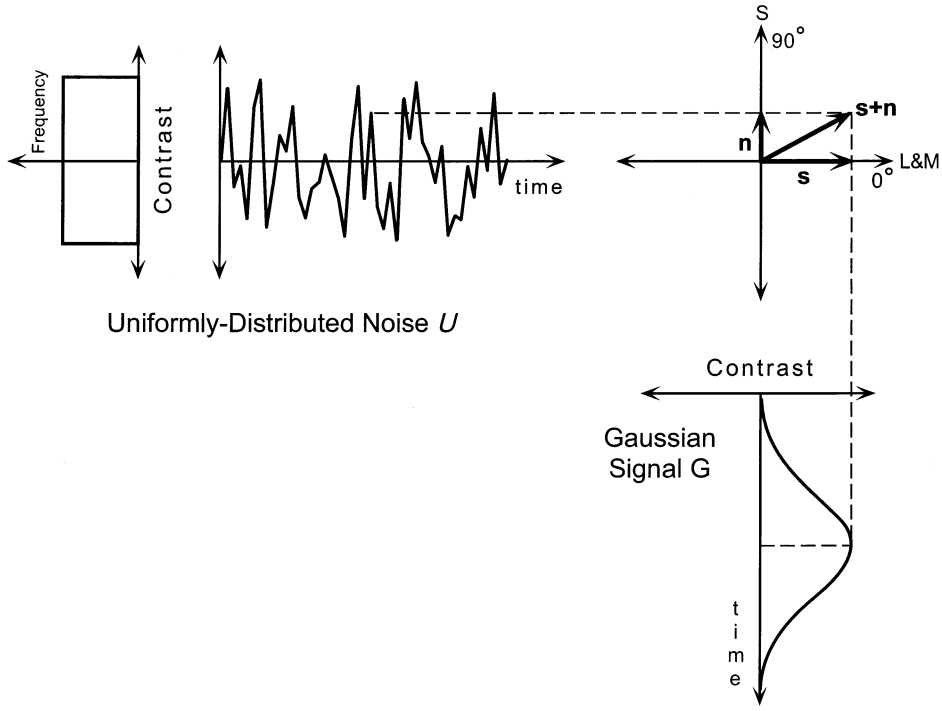

Fig. 3. Combination of signal and axial noise using vector addition [24,26]. Signals (bottom right) are presented with a Gaussian time-course and may vary in the chromatic axis along which they are presented and in their peak contrast. Shown is an equiluminant signal along the 'red' limb of the L and M cone axis (see equiluminant plane at top right). Axial noise samples (top left) are drawn 100 times/s from a uniform density with a maximum contrast under experimental control. The samples are used to modulate chromaticity along an arbitrary chromatic axis; shown is noise along the S cone axis. At any time t the signal $\boldsymbol{s}(t)$ is added to the noise $\boldsymbol{n}(t)$ to generate the instantaneous modulation of chromaticity. The vector addition of signal and noise is shown at the time of the signal peak.

measure of signal strength. The signal diagrammed in Fig. 3 is an equiluminant modulation of the chromaticity of the central patch. The signal in this diagram has an azimuth of 0°, indicated in the color circle by the vector $\boldsymbol{s}$ that corresponds to the maximum contrast of the signal. The azimuth, elevation and peak contrast of the signal were under experimental control.

3.1.2. Noise

Observers measured contrast thresholds for the signals in the absence and in the presence of experimentally added heterochromatic noise. The noise was a rapid, time-varying modulation of the chromaticity of the central Gaussian patch. The noise was used to modulate chromaticity at the field rate of the color monitor, which was run non-interlaced at 100 Hz. The temporal spectral density function of the noise was approximately flat through 50 Hz.

3.1.2.1. Axial noise. The simplest noise used in the experiments was axial noise [24,26]. To generate this noise, samples were drawn randomly from an ensemble described by a uniform density function on some interval $[-a, a]$ centered on zero. The root-mean-square (rms) contrast of the noise could be changed by manipulating the S.D. of the uniform density, which is $1/\sqrt{3}$ of the maximum value a of the density. The samples were used to modulate chromaticity along some specific axis in the color space (hence the term axial noise). In Fig. 3, the noise shown is a modulation along the S cone axis. The average value of the samples is zero, so that the noise shown in Fig. 3 produces random modulation along the S cone axis in both the 90°- and 270°-directions. The chromatic axis and rms contrast of the noise were under experimental control.

During experimental intervals in which noise was used to mask a signal, signal and noise modulations were added together as vectors to produce a modulation that was then added to the gray point **G**. In Fig. 3, the axial noise produces a chromatic modulation that is shown by the vector $\boldsymbol{n}$ in the color circle at the time when the signal reaches its peak. The diagram shows how the chromaticity of the central patch on the monitor at this instant is the vector sum of signal and noise chromaticities at this instant.

This combination of signal and noise can be formalized by writing the sum of signal and noise as a space- and time-dependent chromatic modulation $\boldsymbol{w}(x, t)$. This sum $\boldsymbol{w}$ is a three-dimensional vector in color space and combines the signal modulation $\boldsymbol{s}(x, t)$ and the noise modulation $\boldsymbol{n}(x, t)$:

$$\boldsymbol{w}(x, t) = \boldsymbol{s}(x, t) + \boldsymbol{n}(x, t). \quad (3)$$

The signal chromatic modulation can be separated into temporal and spatial components; writing $S(x)$ for the spatial function that describes the stimulus (a truncated Gaussian centered on the face of the color monitor) and $G(t)$ for the signal temporal function (a truncated Gaussian), one finds

$$\boldsymbol{s}(x, t) = \boldsymbol{s}G(t)S(x) \tag{4a}$$

in which $\boldsymbol{s}$ is the signal chromatic vector. The axial noise may be separated in a similar fashion. Writing $U(t)$ for the process that produces time-dependent samples drawn from a uniform distribution on the interval $[-1, 1]$, one has

$$\boldsymbol{n}(x, t) = \boldsymbol{n}U(t)S(x) \tag{4b}$$

in which $\boldsymbol{n}$ is the noise chromatic vector. The space- and time-dependent chromatic modulation provided by the axial noise masking stimulus is thus described by

$$\boldsymbol{w}(x, t) = \{\boldsymbol{s}G(t) + \boldsymbol{n}U(t)\}S(x). \tag{5}$$

3.1.2.2. Sectored noise. Sectored noise is generated in a way that fills a sector lying in a plane in color space (see Fig. 4). Noise samples that are generated along the chromatic axis of the signal are modulated by an added noise drawn from a uniform, zero-mean distribution along the perpendicular color axis. The latter increases with increasing sample value to form a polar sector of noise.

To generate sectored noise with a half-width θ (see Fig. 4), one uses two random processes that provide samples from uniform distributions on the interval $[-1, 1]$. The first, $U(t)$, is used to provide noise along the chromatic axis of the signal (along which the noise is centered). The second, $U_{\perp}(t)$, is used to provide noise

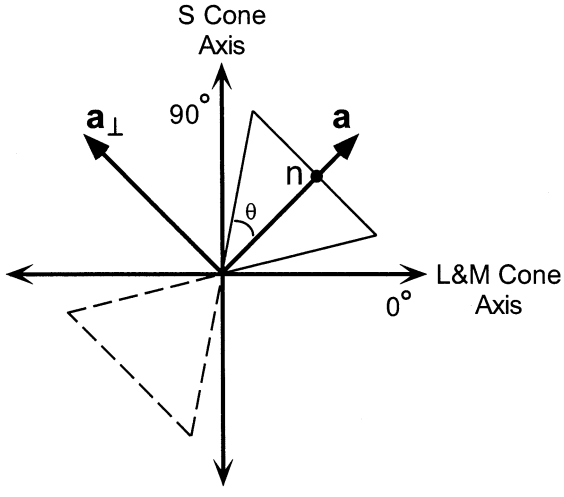

Fig. 4. Sectored noise construction. To zero-mean, uniformly-distributed noise of amplitude n along the signal axis $\boldsymbol{a}$ is added uniformly-distributed noise along the perpendicular axis $\boldsymbol{a}_{\perp}$, modulated by the original noise in such a way as to fill a sector in color space of half-width θ.

along the axis perpendicular to the signal. Calling the unit-length vectors along the chromatic axis of the signal and along the perpendicular axis $\boldsymbol{a}$ and $\boldsymbol{a}_{\perp}$, respectively, one can describe the sectored noise masking stimulus by

$$\boldsymbol{w}(x, t) = \{s\boldsymbol{a}G(t) + nU(t)[\boldsymbol{a} + \tan\theta\ \boldsymbol{a}_{\perp}U_{\perp}(t)]\}S(x), \tag{6}$$

in which s and n are scalars describing signal and noise amplitude.

Sectored noise cannot be distinguished from axial noise along the same central axis by a linear mechanism matched to the central axis: the projections of the noises along the central axis are identical. This can be shown by computing the dot product of the mechanism gradient vector $\boldsymbol{m} = m\boldsymbol{a}$ and the right-hand side of Eq. (6); the noise modulation along the perpendicular axis $\boldsymbol{a}_{\perp}$ produces zero response. By holding constant the noise modulation along the central axis and varying the width of the sector, one can test whether there are departures from such linearity.

Note that the numerical value of the sector half-width angle depends on the choice of basis vectors for the color space. To test for departures from linearity, we compare experimental results, found with some particular set of stimuli, to the results of simulations of detection by alternative models using the same set of stimuli.

3.2. Threshold measurement

Observers used a two-interval forced-choice procedure to measure thresholds for signal detection. In a single run, two independent, interlaced staircases varied signal contrast; the azimuth of the signal and the properties of the noise were held constant from trial to trial. Three correct answers in sequence within a given staircase led to a reduction in contrast on the next presentation of the signal; one incorrect answer led to an increase in signal contrast on the next presentation. Each data point reported below is the average of results from either two or four such staircases, each of length 48 trials.

Single trials comprised two intervals, each starting with a short beep, followed by a pause of 640 ms, and then a stimulus presentation period of duration 640 ms. Observers pressed a switch after the end of the second interval to indicate the interval in which he or she believed the signal to be present. The observer response was followed immediately by indirect feedback in the form of one beep (signal in first interval) or two beeps (signal in second interval). The feedback was followed by an intertrial interval of duration 1 s.

The noise was gated: it appeared only during the presentation intervals. Signal and noise were added at field rate during the intervals in which signal and noise

were present; in the other presentation intervals, the noise was added to a signal of zero contrast. The entire screen was set to the gray point during intervals in which neither signal nor noise were presented.

In summary, the task was to judge during which of two intervals a colored pulse along a fixed chromatic axis was presented; to these signal pulses was added rapid, random chromatic flicker.

4. Results

We used sectored noise to measure the bandwidths of detection mechanisms for signals that appeared yellow, orange, red and violet when presented in isolation. To interpret the data, we relied on the regular effects of axial noise on the detectability of signals along the same chromatic axis. Thresholds rise monotonically with increasing noise rms contrast in a way that was described in earlier visual noise-masking studies [5,24,27–29]. Thresholds for signal detection are unaffected by noise of low rms contrast. At levels that are interpreted by Pelli [28] and Legge et al. [29] to correspond to the intrinsic noise of the detection mechanism, thresholds start to rise in a way that is captured well by assuming a linear relationship between signal energy at threshold E_s and noise energy N:

$$E_s = E_i + kN \tag{7}$$

in which E_i represents the energy of the intrinsic noise and k is a constant. Signal and noise contrasts are related to these energies through a square root operation.

We use this regularity in masking to describe data from experiments in which thresholds are measured as a function of increasing levels of sectored noise. The data collected in sectored noise masking experiments are described well by Eq. (7), and we use the best fits to characterize sensitivity to noise of particular sector widths. The aim is to determine how noise masking depends on sector width. The loss of noise efficacy with increasing sector width is the signature of a narrowband detection mechanism, while independence of masking from sector width characterizes a broadband, linear mechanism.

4.1. Orange signal

The first experiment with sectored noise involved signals along an axis of azimuth 13° in the equiluminant plane. When viewed in isolation, such signals appear orange and appear to have approximately equal amounts of red and yellow when presented at low and moderate contrast levels. The azimuth was chosen by observer MD through trial and error.

Noise-masking functions were measured for each of three observers for sectored noises of half-width 0, 15, 30, 45 and 60°. At half-widths greater than 60°, the stimuli needed to measure noise-masking functions would require lights that lay outside the color gamut of the monitor.

Results for observer FM are shown in Fig. 5. Each data point represents the average of thresholds determined by four staircases; the error bars represent the S.E.M. in these estimates of threshold. The scales along the horizontal noise rms contrast and the vertical signal contrast axes refer to units of contrast to L cones, calculated relative to the gray background.

Data for each sector width are represented by a distinct symbol in Fig. 5. The data points for different sector widths lie atop one another, to a good approximation: masking does not depend on sector width. To quantify the dependence of masking on sector width, the noise-masking model of Eq. (7) was fit to the data for each sector width. The fits were constrained to pass through the same abcissa, namely, to possess the same signal threshold contrast in the absence of noise. The fit curves were used to estimate the amounts of noise that were required to raise threshold threefold. The reciprocals of the amounts of noise needed to raise the threshold by a factor of three provide measures of the sensitivity of the detection mechanism to the noise. These sensitivities are like the field sensitivities in studies of chromatic detection by Stiles [30].

Field sensitivity to noise of varying sector width is plotted in Fig. 6 for the three observers. Each point represents the reciprocal of the level of noise estimated to raise threshold threefold, found through fitting Eq. (7) to data like those in Fig. 5. The result for the signal of azimuth 13° is clear: sensitivity to noise does not depend on sector width, up through half-widths of 60°.

4.2. Alternative detection models

We tried to account for the data using three models. These include models of (i) a linear, broadband mechanism; (ii) non-linear, narrowband mechanisms; and (iii) probability summation between off-axis mechanisms.

4.2.1. Linear detection mechanism

The linear model provides the best-fit, flat lines through the data in Fig. 6. As stated earlier (Section 3.1.2.2), this model predicts that noise masking does not depend on sector width.

One can characterize a linear mechanism within a plane in color space by a series of contours of constant response of the form

$$r = \rho \cos(\phi - \mu) \tag{8}$$

in which the response r to an axial stimulus is determined by the stimulus amplitude ρ, the stimulus direc-

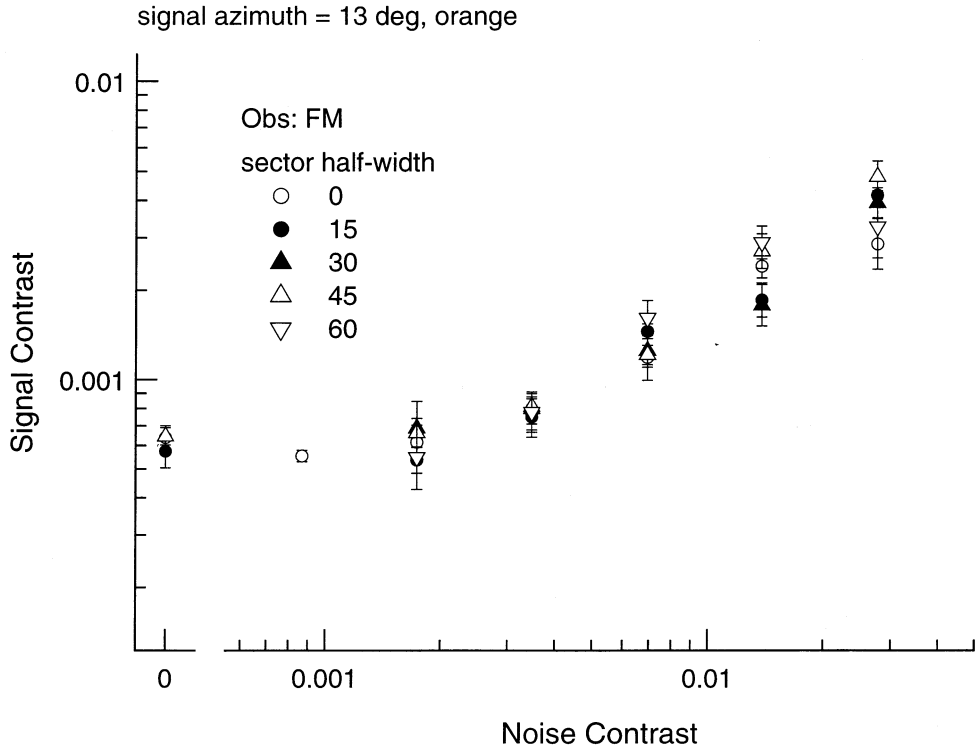

Fig. 5. Sectored noise masking of an orange signal of azimuth 13°. Noise-masking functions were measured for sector half-widths 0, 15, 30, 45 and 60°. Each data point represents the average of four staircases; error bars represent the standard error of the mean. The scales along the horizontal noise rms contrast and vertical signal contrast axes use units of contrast to the L cones. Results for observer FM.

tion ϕ and the mechanism gradient direction μ within the plane [7]. By setting the response r to some constant value, one finds that lights within a response level set are represented by a line in the color plane that is perpendicular to the mechanism gradient μ. Such a set is shown by the curve marked $n = 1$ in Fig. 7.

4.2.2. Narrowband detection mechanisms

A family of non-linear, narrowband mechanisms can be generated by raising the cosine term in Eq. (8) to some exponent greater than one:

$$r = \begin{cases} \rho \cos^n(\phi - \mu), & \text{for } -\frac{\pi}{2} \le \phi - \mu \le \frac{\pi}{2} \\ \rho \left|\cos^n(\phi - \mu)\right|, & \text{for } \frac{\pi}{2} \le \phi - \mu \le \frac{3\pi}{2} \end{cases}. \quad (9)$$

Examples of response level sets for $n = 2$, 5 and 10 are shown in Fig. 7. Increasing the exponent yields increasingly narrowband mechanisms.

The field sensitivities of the linear and the non-linear family of models for the experiment with the signal of azimuth 13° are shown in Fig. 8 by the solid curves. The field sensitivities of the non-linear mechanisms were estimated by a Monte Carlo procedure which is described in Appendix A. The simulations show the expected result: increasing the width of sectored noise produces a less effective noise stimulus for narrowband mechanisms. Furthermore, the decline in noise masking potency with sector width increases as the bandwidth of the detection mechanism decreases. A comparison of Figs. 6 and 8 shows that even for the modest spectral non-linearity produced by squaring, one generates predictions that lie below the range of results found for the three observers.

4.2.3. Probability summation between responses of off-axis mechanisms

If one supposes that there is no mechanism with a peak sensitivity along the signal axis, then the sectored noise must affect detectability through its influence on one or more off-axis mechanisms. We consider the case of two linear off-axis mechanisms and assume that the effect of noise on each off-axis mechanism is proportional to the variance of the noise projected along the gradient direction of the mechanism. We assume that the threshold t for detecting the signal is determined by probability summation between the off-axis mechanisms. If t_1 and t_2 are the thresholds of the first and second off-axis mechanisms, respectively, then Quick's formulation of probability summation using Weibull functions yields the relation:

$$t = (t_1^{-\beta} + t_2^{-\beta})^{-1/\beta}, \quad (10)$$

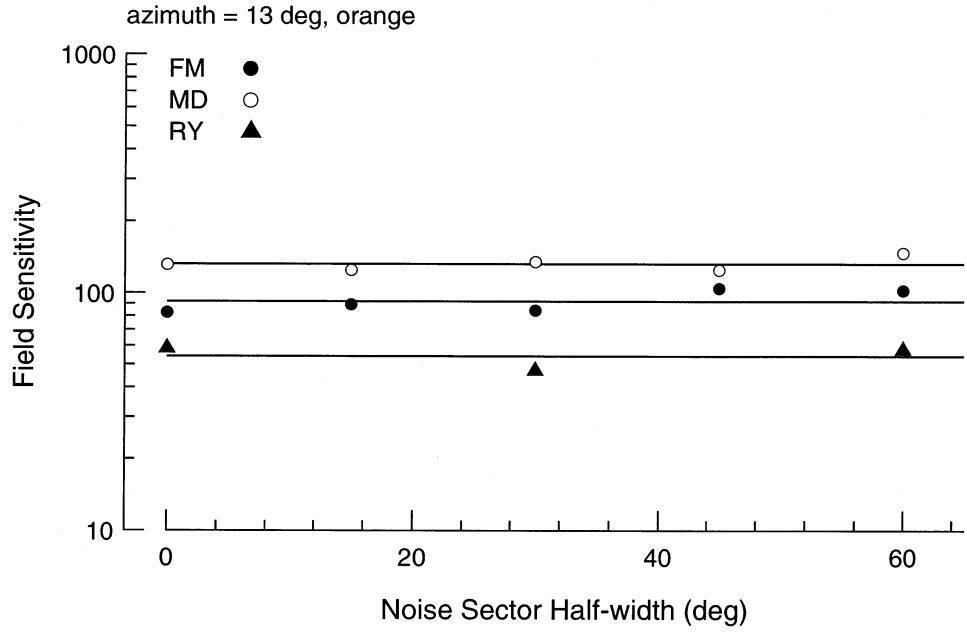

Fig. 6. Sensitivity to noise in an orange signal detection task. Noise sector half-width is plotted along the horizontal axis, while field sensitivity is plotted along the vertical axis. The unit of field sensitivity refers to the absolute value of the reciprocal of the contrast to L cones at estimates of three times threshold, as detailed in the text. Fit horizontal lines correspond to the geometric means of the results for observers FM (filled circles), MD (open circles) and RY (triangles); the last collected data only for half-widths of 0, 30 and 60°.

in which the exponent β determines the amount of probability summation between mechanisms. Here we assume that the exponent β is 2.0. A higher value will affect which off-axis mechanism contributes most to threshold but not how much threshold is elevated by off-axis detection, since this latter quantity is determined by the distribution of noise projected on the mechanism gradients. Taking the square root of both sides of Eq. (7) to find a relation for contrast threshold t in terms of noise variance N, one finds

$$t = E_s^{1/2} = (E_i + kN)^{1/2} \tag{11}$$

and substituting this relation for the terms t_1 and t_2 in Eq. (10), one obtains the following expression for contrast threshold mediated by probability summation between two off-axis mechanisms:

$$t = \left[\frac{(E_{i,1} + k_1N_1)(E_{i,2} + k_2N_2)}{(E_{i,1} + E_{i,2}) + (k_1N_1 + k_2N_2)}\right]^{1/2}. \tag{12}$$

The field sensitivity of this model, for off-axis mechanisms along the L and M cone and the S cone axes, was estimated by a Monte Carlo procedure, which is described in Appendix A. The result of the simulation is shown in Fig. 8 by the dashed curve and shows the expected result: increasing the width of sectored noise leads to changing performance by off-axis mechanisms. Off-axis looking cannot account for the results.

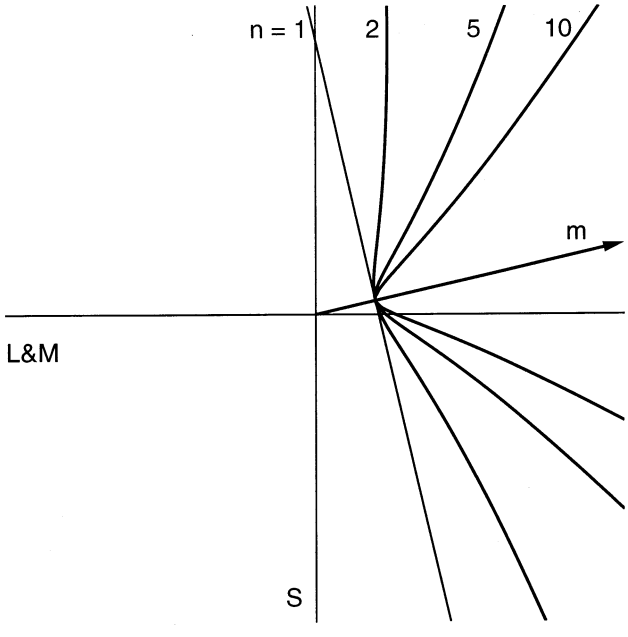

Fig. 7. Response level sets of the cosine-power family of spectral sensitivities. Increasing the exponent yields increasingly narrowband mechanisms, each centered on the gradient vector **m** of the corresponding linear mechanism.

4.3. Yellow, red and violet signals

Do the results obtained for the orange signals hold true for other signals? The results of further experiments, involving signals which appeared yellow, red or violet in isolation, suggest that this is the case. The yellow signal had an azimuth of 33° and was chosen

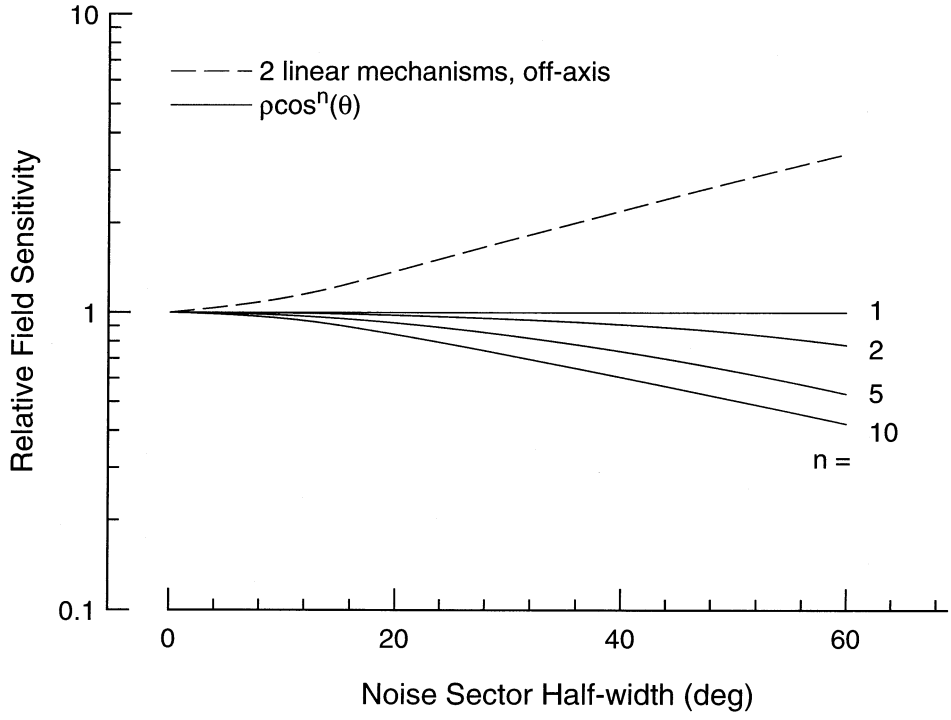

Fig. 8. Predictions of models of spectral sensitivity for the orange signal detection task. Monte Carlo simulations of the effects of sectored noise on (a) narrowband detection mechanisms described by the cosine-power model of Eq. (9) for powers $n = 1$ (linear mechanism), 2, 5 and 10 (lower solid curves) and on (b) two off-axis mechanisms with responses combined by probability summation (uppermost dashed curve). Values computed through simulation at half-widths of 0, 15, 30, 45 and 60° are interpolated by cubic splines to produce the presented curves.

through a process of trial and error to appear unique yellow, namely neither greenish nor reddish, by observer FM. Also chosen by observer FM was the red signal azimuth of 2°, selected for its unique red appearance—neither yellowish nor bluish. The violet azimuth of 315° was chosen by observer MD; signals along this axis appeared about equally red and blue.

Noise masking functions were measured using sectored noise of half-width 0, 30 or 60°. The noise-masking model of Eq. (7) was fit to the data and the parameters were used to estimate the noise rms contrast levels at which thresholds were increased threefold. The reciprocals of these noise contrasts are plotted in Fig. 9 for observers RY (open symbols) and MD (filled symbols) for signals of azimuth 33 (top), 20 (middle) and 315° (bottom).

The field sensitivities for all three signal directions are fit very well by flat lines. There appears to be a slight increase in sensitivity with increasing sector width for the signal of azimuth 33°, for both observers. Yet there is no systematic deviation of the data from the fits of the linear model of the magnitude that would cause us to reject the linear model in favor of either a narrowband model or some model that involves off-axis looking.

5. Discussion

The results for the detection of yellow, orange, red and violet signals show that masking by sectored noise does not depend on the width of the sector. Neither narrowband mechanisms, modelled in this study by the cosine-power family of sensitivities, nor off-axis looking, implemented here through probability summation between two off-axis linear mechanisms, can account for the results.

The simplest and most plausible account of the results is that the visual system possesses spectrally broadband, linear detection mechanisms that are tuned to the signal color directions tested. These signal directions include two that might be expected to isolate standard color-opponent mechanisms, namely the yellow and the red. The signal directions also include the two intermediate directions orange and violet. The results suggest that we possess chromatic detection mechanisms which have preferred azimuths that span a wide range [14]. The wide range of azimuths characterizes the higher-order mechanisms revealed by the habituation studies of Krauskopf and colleagues [2,19] and characterized in further studies by Zaidi and Halevy [31] and Webster and Mollon [32].

In earlier work [24,26], we reported the results of experiments in which axial noise was used to estimate the spectral sensitivities of color detection mechanisms. We discovered a problem with off-axis looking, which is the chromatic analog of off-frequency listening [33] and off-frequency looking [28] in studies of audition and spatial vision, respectively. Off-axis looking can be illustrated by considering the detection of an orange signal. Suppose that the task is to detect a suprathreshold orange signal within axial noise. Noise along the orange axis is an effective masker. Yet if one presents the orange signal within red/blue–green noise from the L and M cone axis, then observers can detect very easily the yellow component of the orange signal. The red noise is a poor masker of the orange signal because the observer uses the yellow detection mechanism. If the orange signal is presented within yellow/blue noise, then observers can readily detect the red component. The yellow noise is a poor masker of the orange signal because observers use the red detection mechanism. It is thus impossible to measure the spectral sensitivity of a putative orange detection mechanism using axial noise, because the optimal strategy for the observer is to use mechanisms with a variety of spectral sensitivities in a noise-dependent fashion.

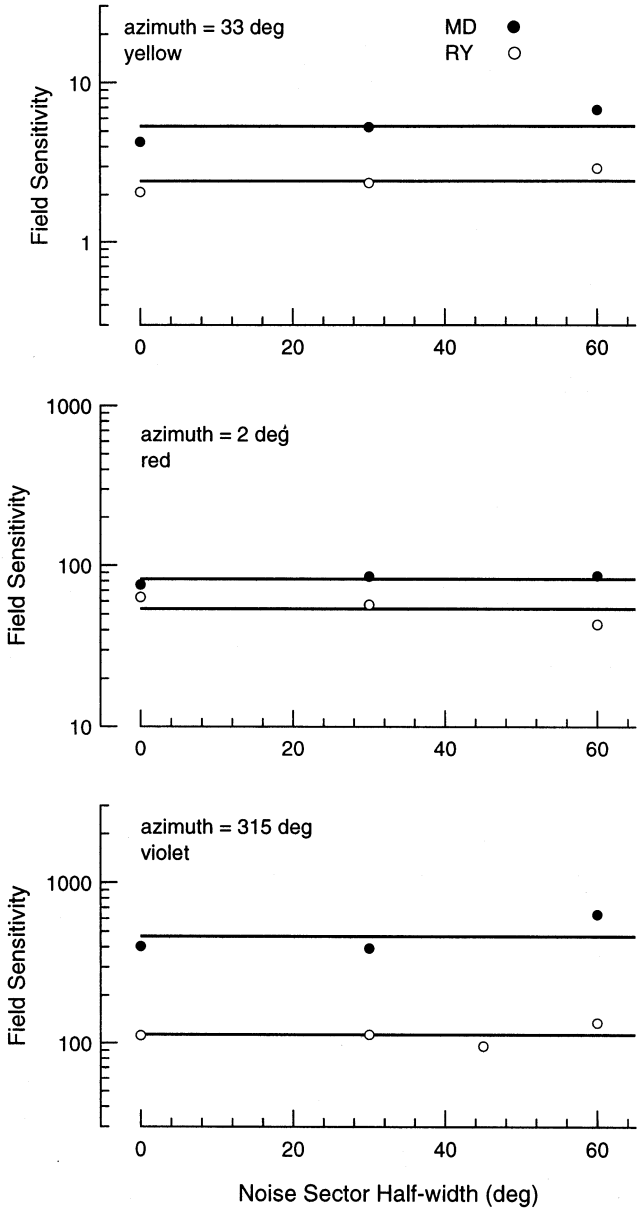

Fig. 9. Sensitivity to noises of varying sector width for yellow, red and violet signals. For the top (yellow), middle (red) and bottom (violet) panels, scale units are contrast to S-cones, L-cones and L-cones, respectively. Fit horizontal lines correspond to the geometric means of the results for RY (open symbols) and MD (filled symbols).

This result for off-axis looking was reproduced using a visual search paradigm [3]. Observers sought a target that was masked by distractors with chromaticities that lay along some axis in color space, so providing an axial noise source. The results showed that observers detect a target of fixed color using a mechanism with a spectral sensitivity that depends on the chromatic axis of the distractors. This is true not only for search for an orange target but also for red and yellow targets [3] and blue and green targets [4].

Indeed, off-axis looking is an optimal strategy for an observer to use in axial noise-masking experiments for signals along all chromatic axes, in cases where the noise lies along an axis that differs from that of the signal (MacLeod, personal communication, 1988). The optimal strategy for observers in axial noise-masking experiments that attempt to measure the spectral sensitivity of a single signal detection mechanism is to use a variety of detection mechanisms. Off-axis looking thus casts doubts on efforts to measure the sensitivities of single color detection mechanisms using axial noise masking [5,24,34–36]. In particular, results that appear to reveal a fixed spectral sensitivity may have involved suboptimal performance by the observers. This problem motivated us to perform the present experiments with sectored noise.

The present results favor the notion that we possess detection mechanisms with sensitivities tuned to intermediate directions of color space. This agrees with the visual search study, which showed that distractors that were presented along an axis orthogonal to that of the signal were completely ineffective [3]. For a signal along an intermediate axis, such distractors should mask detection, if detection were mediated by cardinal axis mechanisms. Yet the distractors did not mask the target at all, suggesting that observers used a detection mechanism which was tuned to the intermediate direction of the signal and insensitive to modulations along the orthogonal (null) axis (as in Fig. 3).

These findings for detection in the equiluminant plane agree with the conclusions of Gegenfurtner and Kiper [5] concerning contrast detection within the plane spanned by the achromatic and the L and M cone axes.

They found that axial noise was most effective when presented along the same axis as the signal and least effective when presented along the orthogonal axis. This held true even for signals along intermediate axes, such as bright red or dark green signals. Their result is inconsistent with detection mediated solely by luminance and chromatic mechanisms.

A clear task for future studies is to move beyond the static measurement of spectral sensitivity to the characterization of the dynamic changes in the spectral sensitivities of detection mechanisms that observers are able to deploy.

Acknowledgements

We thank Karl Gegenfurtner, John Krauskopf, Peter Lennie, Donald MacLeod, George Sperling and an anonymous referee for their helpful comments and criticisms. We thank also Professor Bernard Laget, Director of the Institut d'Ingéniérie de la Vision at the Université Saint-Etienne, for his support. We thank Françoise Maingueneau and Rosa Yssaad for their help with the observations. Germinal phases of this work were supported by National Eye Institute grant EY01319 to Peter Lennie. This work was supported by National Eye Institute grant EY10014 and by a Bourse d'Accueil from the Région Rhône-Alpes to M. D'Zmura.

Appendix A. Monte Carlo simulation of model sensitivities

The field sensitivities of the non-linear, narrowband mechanisms described by the cosine-power model of Eq. (9) and the off-axis mechanisms combined by probability summation were estimated through a Monte Carlo procedure. In all cases, 10000 random noise vectors were generated for sector half-widths of 0, 15, 30, 45 and 60°.

For each of the narrowband mechanisms, the response distributions for each half-width were calculated for a mechanism peak direction of azimuth 13°, matching that of the signal. The variance of each distribution was then used with the noise-masking model of Eq. (7) to calculate the noise energy needed to raise signal threshold threefold above its level in the absence of noise. The values for the intrinsic noise E_{i} and the constant k in Eq. (7) were estimated using the average values found for the three observers in this study. These values are not critical to the results of the simulation, which are shown in Fig. 8 by the solid curves for $n = 2$, 5 and 10. Cubic splines were fit to the simulated values to generate the curves.

To estimate field sensitivity for the off-axis mechanisms, note that if the external noise variance N is set to zero, then Eq. (12) reduces to

$$t = \left[\frac{E_{i,1}E_{i,2}}{E_{i,1} + E_{i,2}}\right]^{1/2} \tag{A1}$$

By taking the ratio of Eq. (12) to Eq. (A1) and setting it to 3.0, one can use a simple root finding algorithm to solve for the amount of noise that raises threshold 3-fold. The results of the simulation are shown in Fig. 8 by the dashed curve.

References

[1] Hurvich LM, Jameson D. An opponent-process theory of color vision. Psychol Rev 1957;64:384–404.
[2] Krauskopf J, Williams DR, Mandler M, Brown A. Higher-order color mechanisms. Vis Res 1986;26:23–32.
[3] D'Zmura M. Color in visual search. Vis Res 1991;31:951–66.
[4] Bauer B, Jolicoeur P, Cowan WB. Visual search for colour targets that are or are not linearly separable from distractors. Vis Res 1996;36:1439–65.
[5] Gegenfurtner KR, Kiper DC. Contrast detection in luminance and chromatic noise. J Opt Soc Am A 1992;9:1880–8.
[6] DeValois RL, Abramov I, Jacobs GH. Analysis of response patterns of LGN cells. J Opt Soc Am 1966;56:966–77.
[7] Derrington AM, Krauskopf J, Lennie P. Chromatic mechanisms in lateral geniculate nucleus of macaque. J Physiol Lond 1984;357:241–65.
[8] Lennie P, Krauskopf J, Sclar G. Chromatic mechanisms in striate cortex of macaque. J Neurosci 1990;10:649–69.
[9] DeValois RL, Cottaris N, Elfar S. S-cone inputs to striate cortex cells. Invest Ophthalmol Vis Sci 1997;38:15.
[10] Kiper, DC, Fenstemaker, SB, Gegenfurtner, KR. Chromatic properties of neurons in macaque area V2. Vis Neurosci 1997, in press.
[11] Gegenfurtner KR, Kiper DC, Levitt JB. Functional properties of neurons in macaque area V3. J Neurophysiol 1997;77:1906–23.
[12] Fletcher H. Auditory patterns. Rev Mod Phys 1940;12:47–65.
[13] Stromeyer CF III, Julesz B. Spatial-frequency masking in vision: critical bands and spread of masking. J Opt Soc Am 1972;62:1221–32.
[14] D'Zmura M, Lennie P. Mechanisms of color constancy. J Opt Soc Am A 1986;3:1662–72.
[15] D'Zmura M, Knoblauch K. Spectral bandwidths of color detection mechanisms. Perception Suppl 1996;25:15.
[16] Knoblauch K, D'Zmura M. Spectral bandwidths of color mechanisms evaluated with sectored noise. Invest Ophthalmol Vis Sci 1997;38:255.
[17] MacLeod DIA, Boynton RM. Chromaticity diagram showing cone excitation by stimuli of equal luminance. J Opt Soc Am 1979;69:1183–6.
[18] Brainard D. Cone contrast and opponent modulation color spaces. In: Kaiser P, Boynton RM, editors. Human Color Vision, 2nd edn. Washington, DC: Optical Society of America, 1996:563–79.
[19] Krauskopf J, Williams DR, Heeley DW. Cardinal directions of color space. Vis Res 1982;22:1123–31.
[20] Wyszecki G, Stiles WS. Color Science. Concepts and Methods, Quantitative Data and Formulae, 2nd edn. New York: Wiley, 1982.

[21] Smith VC, Pokorny J. Spectral sensitivity of the foveal cone photopigments between 400 and 500 nm. Vis Res 1975;15:161–71.
[22] Hassenstein B. Modellrechnung zur datenverarbeitung beim farbensehen des menschen. Kybernetik 1968;4:209–23.
[23] Jameson D, Hurvich LM. Opponent response functions related to measured cone photopigments. J Opt Soc Am 1968;58:429–30.
[24] D'Zmura, M. Surface color psychophysics. PhD Dissertation, University of Rochester, New York, 1990.
[25] Knoblauch K. Dual bases in dichromatic color space. In: Drum B, editor. Colour Vision Deficiencies XII. Dordrecht: Kluwer, 1995:165–76.
[26] D'Zmura M, Krauskopf J, Lennie P. Hue selectivity revealed by heterochromatic noise masking. Invest Ophthalmol Vis Sci Suppl 1987;28:92.
[27] Nagaraja NS. Effect of luminance noise on contrast thresholds. J Opt Soc Am 1964;54:950–5.
[28] Pelli, D. The effects of visual noise. PhD Dissertation, Cambridge University, Cambridge, 1981.
[29] Legge GE, Kersten D, Burgess AE. Contrast discrimination in noise. J Opt Soc Am A 1987;4:391–404.
[30] Stiles WS. Mechanisms of Colour Vision. New York: Academic Press, 1978.
[31] Zaidi Q, Halevy D. Visual mechanisms that signal the direction of color changes. Vis Res 1993;33:1037–51.
[32] Webster MA, Mollon JD. The influence of contrast adaptation on color appearance. Vis Res 1994;34:1993–2020.
[33] Patterson RD, Nimmo-Smith I. Off-frequency listening and auditory-filter asymmetry. J Acoust Soc Am 1980;67:229–45.
[34] Li A, Lennie P. Mechanisms underlying segmentation of colored textures. Vis Res 1997;37:83–97.
[35] Giulianini, F, Eskew, RT, Jr. Chromatic masking in the (L-, M-) plane of cone–contrast space reveals only two detection mechanisms. Preprint, 1997.
[36] Sankarelli, MJ, Mullen, KT. Postreceptoral chromatic detection mechanisms revealed by noise masking in three-dimensional cone contrast space. J Opt Soc Am A 1997, in press.